Mathematical Biosciences and Engineering

http://www.aimspress.com/journal/mbe

MBE, 21(8): 6898–6914.
DOI: 10.3934/mbe.2024302
Received: 15 May 2024
Revised: 26 July 2024
Accepted: 14 August 2024
Published: 21 August 2024

Research article

A neural network model for goat gait

Liqin Liu and Chunrui Zhang*

Department of Mathematics, Northeast Forestry University, Harbin 150040, China

* **Correspondence:** Email: math@nefu.edu.cn; Tel: +86045182190543.

Abstract: In this paper, our main objective was to investigate the central pattern generator (CPG) neural network model for quadruped gait with time delay. First, we computed the normal form of the model on the center manifold, the bifurcation direction, and stability conditions of the bifurcating periodic solutions. Second, we applied the CPG model for quadruped gait to obtain reference models for goat's diagonal trotting gait on the flat ground and walking gait on the 18 degree slope through the trust region inversion algorithm. Finally, we performed numerical simulations to support theoretical analysis.

Keywords: time delay neural network; quadruped gait CPG model; Hopf bifurcation; goat gait

1. Introduction

Animal gaits are a rhythmic behavior controlled by central pattern generator (CPG), which generates rhythmic signals to the muscle groups of animals, controls their own rhythmic movements, and produces various gaits in animal locomotion. From a biological perspective, CPG is a distributed vibration network composed of neurons in the central nervous system of animals. Human beings get inspiration from the organizational structure, movement mechanism, and behavior of biological bodies, and constantly learn and imitate the characteristics and functions of certain organisms, thereby improving their adaptability to nature and making contributions to the development of science and technology. Therefore, biologists and mathematicians have established some CPG biological and mathematical models by imitating the neural network patterns of animal CPG. Golubitsky et al. [1] has investigated a composition pattern of CPG neurons in quadrupedal gaits and obtained a new primary gait "jump". The animal gait network proposed by Buono et al. [2] can generate six primary gaits: walk, trot, pace, bound, pronk, and jump. Furthermore, based on the primary gait, the phase patterns of transverse gallop and rotary gallop in quadruped secondary gait were provided [3]. The present authors have studied CPG neural network models for the primary gait of quadrupeds [4, 5].

Animal gait CPG neural networks have wide applications. Inspired by animal movements, in the

gait planning of biomimetic robots, a CPG model is set for the robot system by imitating the CPG network of animals in nature. By utilizing the coupling between oscillators in the CPG model, periodic oscillation signals are generated to achieve stable rhythmic gait behavior of the robot. For instance, the CPG network can be used to construct gait networks for hexapod robots gait networks [6, 7] and quadruped robots gait networks [8–10]. In article [11], a method for designing a robot system controller was proposed using a CPG control network, and in article [12], the robot gait was produced based on animal gait. In [13], a CPG animation model was constructed using the CPG network system.

In quadruped mammals, goats have smaller bodies and stronger bones in their limbs, and their hindlimbs are stronger than their forelimbs specifically. Goats have a brisk and agile gait when walking, and they can walk freely, flexibly, and quickly on the ground, slopes, steep walls and uneven surfaces. Moreover, they can also walk long distances and have good road adaptability and obstacle crossing ability. Goats are less restricted by the environment and, therefore, goat gaits have certain research value. In literature [14], the author used goats as the research object and conducted kinematic analysis on the multimode gait of goats on conventional and unconventional roads. In work [15], the author analyzed the gait of goats from the perspective of structural bionics. At present, there is little research on mathematical models of goat gaits to our knowledge. In this paper, we deal with this problem and propose the CPG neural network models of goat gaits from a mathematical perspective. We study the following model given in [5]

$$\begin{cases} \dot{x}_1(t) = ax_1(t) + b\tanh(x_1(t)) + d\tanh(x_7(t)) + c\tanh(x_2(t-\tau)), \\ \dot{x}_2(t) = ax_2(t) + b\tanh(x_2(t)) + d\tanh(x_8(t)) + c\tanh(x_1(t-\tau)), \\ \dot{x}_3(t) = ax_3(t) + b\tanh(x_3(t)) + d\tanh(x_1(t)) + c\tanh(x_4(t-\tau)), \\ \dot{x}_4(t) = ax_4(t) + b\tanh(x_4(t)) + d\tanh(x_2(t)) + c\tanh(x_3(t-\tau)), \\ \dot{x}_5(t) = ax_5(t) + b\tanh(x_5(t)) + d\tanh(x_3(t)) + c\tanh(x_6(t-\tau)), \\ \dot{x}_6(t) = ax_6(t) + b\tanh(x_6(t)) + d\tanh(x_4(t)) + c\tanh(x_5(t-\tau)), \\ \dot{x}_7(t) = ax_7(t) + b\tanh(x_7(t)) + d\tanh(x_5(t)) + c\tanh(x_8(t-\tau)), \\ \dot{x}_8(t) = ax_8(t) + b\tanh(x_8(t)) + d\tanh(x_6(t)) + c\tanh(x_7(t-\tau)), \end{cases} \tag{1.1}$$

where a, b, c, d are constants and $\tau \geq 0$ is the time delay. The state variable $(x_1(t), x_2(t), \cdots, x_8(t))$ is the output signal from the CPG to the legs, where $x_1(t)$ and $x_7(t)$ are the output signals to the left hind leg, $x_3(t)$ and $x_5(t)$ are the output signals to the left fore leg, $x_2(t)$ and $x_8(t)$ are the output signals to the right hind leg, and $x_4(t)$ and $x_6(t)$ are the output signals to the right fore leg. The network diagram of system (1.1) is shown in Figure 1.

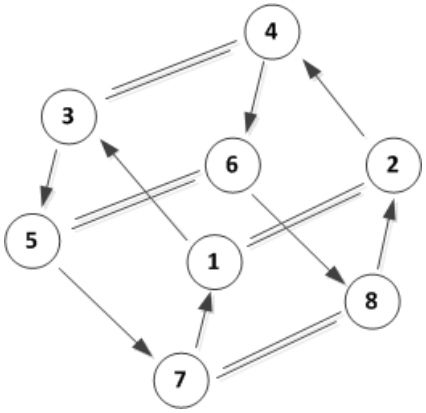

Figure 1. Schematic diagram of the system (1.1).

In reference [5], the authors give the conditions $(H1) : |c| > |a + b + d| \; if \; (a + b)d > 0$, $(H2) : |c| > |a + b - d| \; if \; (a + b)d < 0$, and critical values $\tau_j^k (j = 1, 2, 3, 4, 5, 6, 7, 8)$ (see Table 1 in [5]) for the Hopf bifurcations of the model (1.1) at the zero equilibrium.

The main objective of this paper is to provide further the bifurcation direction and stability conditions of the bifurcating periodic solutions of the model (1.1). Based on the model (1.1), the CPG neural network models of goat gaits are given by using the parameter inversion algorithm.

2. Normal form for Hopf bifurcation

In this section, we use the method in reference [16] to calculate the normal forms of Hopf bifurcations on the center manifold of the Eq (1.1) at the zero equilibrium. Normalizing the delay τ by the time-scaling $t \mapsto \frac{t}{\tau}$, Eq (1.1) can be rewritten as a functional differential equation in $C = C([-1, 0], R^8)$,

$$\begin{cases} \dot{u}_1(t) = \tau(au_1(t) + b\tanh(u_1(t)) + d\tanh(u_7(t)) + c\tanh(u_2(t-1))), \\ \dot{u}_2(t) = \tau(au_2(t) + b\tanh(u_2(t)) + d\tanh(u_8(t)) + c\tanh(u_1(t-1))), \\ \dot{u}_3(t) = \tau(au_3(t) + b\tanh(u_3(t)) + d\tanh(u_1(t)) + c\tanh(u_4(t-1))), \\ \dot{u}_4(t) = \tau(au_4(t) + b\tanh(u_4(t)) + d\tanh(u_2(t)) + c\tanh(u_3(t-1))), \\ \dot{u}_5(t) = \tau(au_5(t) + b\tanh(u_5(t)) + d\tanh(u_3(t)) + c\tanh(u_6(t-1))), \\ \dot{u}_6(t) = \tau(au_6(t) + b\tanh(u_6(t)) + d\tanh(u_4(t)) + c\tanh(u_5(t-1))), \\ \dot{u}_7(t) = \tau(au_7(t) + b\tanh(u_7(t)) + d\tanh(u_5(t)) + c\tanh(u_8(t-1))), \\ \dot{u}_8(t) = \tau(au_8(t) + b\tanh(u_8(t)) + d\tanh(u_6(t)) + c\tanh(u_7(t-1))). \end{cases} \tag{2.1}$$

Denoting $U = (u_1, u_2, u_3, u_4, u_5, u_6, u_7, u_8)^T$, $U_t = U(t + \theta), U_t \in C$, where $\theta \in [-1, 0]$. Let $\tau = \tau_{2j}^0 + \mu$ $(j = 1, 2, 3, 4)$, for μ is a bifurcation parameter, then Eq (2.1) can further be written as the following form:

$$\dot{U}(t) = L(0)U_t + F(U_t, \mu), \tag{2.2}$$

where

$$F(U_t, \mu) = (L(\mu) - L(0))U_t + F_0(U_t, \mu),$$

$$L(\mu)\varphi = (\tau_{2j}^0 + \mu)\begin{pmatrix} (a+b)(\varphi_1(0)) + d\varphi_7(0) + c\varphi_2(-1) \\ (a+b)(\varphi_2(0)) + d\varphi_8(0) + c\varphi_1(-1) \\ (a+b)(\varphi_3(0)) + d\varphi_1(0) + c\varphi_4(-1) \\ (a+b)(\varphi_4(0)) + d\varphi_2(0) + c\varphi_3(-1) \\ (a+b)(\varphi_5(0)) + d\varphi_3(0) + c\varphi_6(-1) \\ (a+b)(\varphi_6(0)) + d\varphi_4(0) + c\varphi_5(-1) \\ (a+b)(\varphi_7(0)) + d\varphi_5(0) + c\varphi_8(-1) \\ (a+b)(\varphi_8(0)) + d\varphi_6(0) + c\varphi_7(-1) \end{pmatrix},$$

and

$$F_0(U_t,\mu) = (\tau_{2j}^0 + \mu)\begin{pmatrix} -\frac{b}{3}\varphi_1^3(0) - \frac{d}{3}\varphi_7^3(0) - \frac{c}{3}\varphi_2^3(-1) \\ -\frac{b}{3}\varphi_2^3(0) - \frac{d}{3}\varphi_8^3(0) - \frac{c}{3}\varphi_1^3(-1) \\ -\frac{b}{3}\varphi_3^3(0) - \frac{d}{3}\varphi_1^3(0) - \frac{c}{3}\varphi_4^3(-1) \\ -\frac{b}{3}\varphi_4^3(0) - \frac{d}{3}\varphi_2^3(0) - \frac{c}{3}\varphi_3^3(-1) \\ -\frac{b}{3}\varphi_5^3(0) - \frac{d}{3}\varphi_3^3(0) - \frac{c}{3}\varphi_6^3(-1) \\ -\frac{b}{3}\varphi_6^3(0) - \frac{d}{3}\varphi_4^3(0) - \frac{c}{3}\varphi_5^3(-1) \\ -\frac{b}{3}\varphi_7^3(0) - \frac{d}{3}\varphi_5^3(0) - \frac{c}{3}\varphi_8^3(-1) \\ -\frac{b}{3}\varphi_8^3(0) - \frac{d}{3}\varphi_6^3(0) - \frac{c}{3}\varphi_7^3(-1) \end{pmatrix} + h.o.t.,$$

where $\varphi = (\varphi_1, \varphi_2, \varphi_3, \varphi_4, \varphi_5, \varphi_6, \varphi_7, \varphi_8)^T \in C$. By the Riesz representation theorem, there is $\eta(\theta,\mu)$, such that $L(\mu)\varphi = \int_{-1}^{0} d\eta(\theta,\mu)\varphi(\theta)$, and we select $\eta(\theta,\mu) = (\tau_{2j}^0 + \mu)(A\delta(\theta) + B\delta(\theta+1))$, where

$$A = \begin{pmatrix} B_0 & 0 & 0 & D_0 \\ D_0 & B_0 & 0 & 0 \\ 0 & D_0 & B_0 & 0 \\ 0 & 0 & D_0 & B_0 \end{pmatrix}, B = \begin{pmatrix} C_0 & 0 & 0 & 0 \\ 0 & C_0 & 0 & 0 \\ 0 & 0 & C_0 & 0 \\ 0 & 0 & 0 & C_0 \end{pmatrix},$$

$$B_0 = \begin{pmatrix} a+b & 0 \\ 0 & a+b \end{pmatrix}, D_0 = \begin{pmatrix} d & 0 \\ 0 & d \end{pmatrix}, C_0 = \begin{pmatrix} 0 & c \\ c & 0 \end{pmatrix}.$$

The Taylor expansion of $F(U_t,\mu)$ is denoted as

$$F(U_t,\mu) = \frac{1}{2!}F_2(\varphi,\mu) + \frac{1}{3!}F_3(\varphi,\mu) + h.o.t.$$

with

$$F_2(\varphi,\mu) = \mu\begin{pmatrix} (a+b)(\varphi_1(0)) + d\varphi_7(0) + c\varphi_2(-1) \\ (a+b)(\varphi_2(0)) + d\varphi_8(0) + c\varphi_1(-1) \\ (a+b)(\varphi_3(0)) + d\varphi_1(0) + c\varphi_4(-1) \\ (a+b)(\varphi_4(0)) + d\varphi_2(0) + c\varphi_3(-1) \\ (a+b)(\varphi_5(0)) + d\varphi_3(0) + c\varphi_6(-1) \\ (a+b)(\varphi_6(0)) + d\varphi_4(0) + c\varphi_5(-1) \\ (a+b)(\varphi_7(0)) + d\varphi_5(0) + c\varphi_8(-1) \\ (a+b)(\varphi_8(0)) + d\varphi_6(0) + c\varphi_7(-1) \end{pmatrix},$$

$$F_3(\varphi,\mu)=\tau_{2j}^0\begin{pmatrix} -\frac{b}{3}\varphi_1^3(0)-\frac{d}{3}\varphi_7^3(0)-\frac{c}{3}\varphi_2^3(-1)\\ -\frac{b}{3}\varphi_2^3(0)-\frac{d}{3}\varphi_8^3(0)-\frac{c}{3}\varphi_1^3(-1)\\ -\frac{b}{3}\varphi_3^3(0)-\frac{d}{3}\varphi_1^3(0)-\frac{c}{3}\varphi_4^3(-1)\\ -\frac{b}{3}\varphi_4^3(0)-\frac{d}{3}\varphi_2^3(0)-\frac{c}{3}\varphi_3^3(-1)\\ -\frac{b}{3}\varphi_5^3(0)-\frac{d}{3}\varphi_3^3(0)-\frac{c}{3}\varphi_6^3(-1)\\ -\frac{b}{3}\varphi_6^3(0)-\frac{d}{3}\varphi_4^3(0)-\frac{c}{3}\varphi_5^3(-1)\\ -\frac{b}{3}\varphi_7^3(0)-\frac{d}{3}\varphi_5^3(0)-\frac{c}{3}\varphi_8^3(-1)\\ -\frac{b}{3}\varphi_8^3(0)-\frac{d}{3}\varphi_6^3(0)-\frac{c}{3}\varphi_7^3(-1)\end{pmatrix}.$$

Expanding space C to $BC=\{\varphi:[-1,0]\to C^8|\ \varphi$ is continuous on [-1,0) and $\lim_{\theta\to 0^-}\varphi(\theta)\in C^8\}$. The element of BC can be expressed as $\upsilon=\varphi+X_0\nu,\varphi\in C,\nu\in C^8$, and

$$X_0(\theta)=\begin{cases}0, & -1\le\theta<0\\ I, & \theta=0\end{cases}$$

with I as the identity matrix.

For $\phi\in C^1=C^1([-1,0],C^8)$, we define

$$A_0\phi=\begin{cases}\dot{\phi}, & -1\le\theta<0\\ \int_{-1}^0 d\eta(\theta,0)\phi(\theta), & \theta=0.\end{cases}\tag{2.3}$$

For $\psi\in C^{1^*}=C^1([-1,0],C^{8^*})$, the adjoint operator of A_0 is

$$A_0^*\psi=\begin{cases}-\dot{\psi}, & -1\le s<0,\\ \int_{-1}^0\psi(-s)d\eta(s,0), & s=0,\end{cases}\tag{2.4}$$

and a bilinear inner product is the following:

$$<\psi,\phi>=\bar{\psi}(0)\phi(0)-\int_{-1}^0\int_0^\theta\bar{\psi}(\xi-\theta)d\eta(\theta,0)\phi(\xi)d\xi.\tag{2.5}$$

Let $\Phi(\theta)$ and $\Psi(s)$ be the eigenvectors corresponding to the eigenvalues $i\omega_j\tau_{2j}^0$ and $-i\omega_j\tau_{2j}^0$, respectively. Note that $\Phi(\theta)=(\phi(\theta),\bar{\phi}(\theta))$, $\Psi(s)=(\bar{\psi}(s),\psi(s))^T$ with $\dot{\Phi}=\Phi(\theta)J,\dot{\Psi}(s)=-J\Psi(s),<\Psi(s),\Phi(\theta)>=I$, and $J=diag(i\omega_j\tau_{2j}^0,-i\omega_j\tau_{2j}^0)$. It can be easily calculated from (2.3) and (2.4) that

$$\phi(\theta)=(1,-1,1,-1,1,-1,1,-1)^Te^{i\omega_j\tau_{2j}^0\theta},$$

$$\psi(s)=D(-1,1,-1,1,-1,1,-1,1)e^{i\omega_j\tau_{2j}^0 s}.$$

Hence, we obtain $D=\frac{1}{8(-1+ce^{i\omega_j\tau_{2j}^0})}$ from $<\phi(s),\phi(\theta)>=1$.

Let P be a vector space expanded by $\phi(\theta)$ and $\bar{\phi}(\theta)$, P^* be a vector space expanded by $\phi(s)$ and $\bar{\phi}(s)$, then C can be decomposed as $C=P\oplus Q$, where $Q=\{\phi\in C:<\psi,\phi>=0,\forall\psi\in P^*\}$. Define mapping $\Pi:BC\to P$ as $\Pi(\varphi+X_0\nu)=\Phi[(\psi,\phi)+\psi(0)\nu]$ and $Q^1=ker\pi\bigcap C^1$.

Using the decomposition of $U=\Phi x+y$ with $x=(x_1,x_2)^T,y=(y_1,y_2,y_3,y_4,y_5,y_6,y_7,y_8)^T$, system (2.1) can be decomposed as

$$\begin{cases}\dot{x}=Jx+\Psi(0)F(\Phi x+y,\mu),\\ \dot{y}=A_{Q^1}y+(I-\Pi)X_0F(\Phi x+y,\mu).\end{cases}\tag{2.6}$$

We have the Taylor expansion as follows:

$$\begin{cases} \dot{x} = Jx + \frac{1}{2!}f_2^1(x,y,\mu) + \frac{1}{3!}f_3^1(x,y,\mu) + h.o.t., \\ \dot{y} = A_{Q^1}y + \frac{1}{2!}f_2^2(x,y,\mu) + \frac{1}{3!}f_3^2(x,y,\mu) + h.o.t., \end{cases} \tag{2.7}$$

where

$$f_2^1(x,y,\mu) = \Psi(0)F_2(\Phi x + y, \mu),\ f_3^1(x,y,\mu) = \Psi(0)F_3(\Phi x + y, \mu),$$
$$f_2^2(x,y,\mu) = (I-\Pi)X_0F_2(\Phi x + y, \mu),\ f_3^2(x,y,\mu) = (I-\Pi)X_0F_3(\Phi x + y, \mu).$$

Normal form of Eq (2.7) on the center manifold at the origin is given by

$$\dot{x} = Jx + \frac{1}{2!}g_2^1(x,0,\mu) + \frac{1}{3!}g_3^1(x,0,\mu) + h.o.t., \tag{2.8}$$

where

$$g_2^1(x,\ 0,\ \mu) = \mathrm{Proj}_{\ker(M_2^1)}f_2^1(x,0,\mu),$$
$$g_3^1(x,\ 0,\ \mu) = \mathrm{Proj}_{\ker(M_3^1)}\tilde{f}_3^1(x,0,\mu),$$
$$\ker(M_2^1) = span\{\begin{pmatrix} \mu x_1 \\ 0 \end{pmatrix}, \begin{pmatrix} 0 \\ \mu x_2 \end{pmatrix}\},$$
$$\ker(M_3^1) = span\{\begin{pmatrix} \mu^2 x_1 \\ 0 \end{pmatrix}, \begin{pmatrix} x_1^2 x_2 \\ 0 \end{pmatrix}, \begin{pmatrix} 0 \\ \mu^2 x_2 \end{pmatrix}, \begin{pmatrix} 0 \\ x_1 x_2^2 \end{pmatrix}\},$$
$$\tilde{f}_3^1(x,0,\mu) = f_3^1(x,0,\mu) + \frac{3}{2}[(D_x f_2^1)U_2^1(x,\mu) + [(D_y f_2^1)h]U_2^2(x,\mu),$$
$$U_2^1(x,\mu)_{\mu=0} = (M_2^1)^{-1}\mathrm{Proj}_{\mathrm{Im}(M_2^1)}f_2^1(x,0,0),\ M_2^2U_2^2(x,\mu) = f_2^2(x,0,\mu).$$

After calculating, we obtain

$$\frac{1}{2!}g_2^1(x,0,\mu) = \begin{pmatrix} \bar{a}_1\mu x_1 \\ a_1\mu x_2 \end{pmatrix},$$

where $a_1 = 8D(-a-b-d+ce^{i\omega_j\tau_{2j}^0})$.

In the following, we can compute the cubic terms $\frac{1}{3!}g_3^1(x,0,\mu)$ as

$$\begin{aligned} \frac{1}{3!}g_3^1(x,0,\mu) &= \frac{1}{3!}\mathrm{Proj}_{\ker(M_3^1)}\tilde{f}_3^1(x,0,\mu) \\ &= \frac{1}{3!}\mathrm{Proj}_S\tilde{f}_3^1(x,0,0) + O(\mu^2|x|) \\ &= \frac{1}{3!}\mathrm{Proj}_S f_3^1(x,0,\mu) + \frac{1}{4}\mathrm{Proj}_S[(D_x f_2^1)(x,0,0)U_2^1(x,0) + (D_y f_2^1)(x,0,0)U_2^2(x,0)] \\ &+ O(\mu^2|x|), \end{aligned}$$

with

$$S = span\{\begin{pmatrix} x_1^2 x_2 \\ 0 \end{pmatrix}, \begin{pmatrix} 0 \\ x_1 x_2^2 \end{pmatrix}\}.$$

Since $f_2^1(x,0,0) = (0,0)^T$, $f_2^1(x,y,0) = (0,0)^T$, we obtain $U_2^1(x,0) = (0,0)^T$, $(D_y f_2^1)(x,0,0) = (0,0)^T$,

thus

$$\frac{1}{3!}g_3^1(x,0,\mu) = \frac{1}{3!}\text{Proj}_S f_3^1(x,0,0) + O(\mu^2|x|)$$
$$= \begin{pmatrix} \bar{a}_2 x_1^2 x_2 \\ a_2 x_1 x_2^2 \end{pmatrix} + O(\mu^2|x|),$$

where $a_2 = -8\tau_{2j}^0 D(-b + ce^{i\omega_i\tau_{2j}^0} - d)$.

Then, the normal form (2.8) can be written as

$$\begin{cases} \dot{x_1} = i\omega_i\tau_{2j}^0 x_1 + \bar{a}_1\mu x_1 + \bar{a}_2 x_1^2 x_2 + h.o.t., \\ \dot{x_2} = -i\omega_i\tau_{2j}^0 x_2 + a_1\mu x_2 + a_2 x_1 x_2^2 + h.o.t.. \end{cases} \tag{2.9}$$

By transforming the variables $x_1 = w_1 + iw_2$, $x_2 = w_1 - iw_2$ and $w_1 = rcos\xi$, $w_2 = rsin\xi$, Eq (2.9) can be written as

$$\begin{cases} \dot{r} = k_1\mu r + k_2 r^3 + h.o.t, \\ \dot{\xi} = -\omega_j\tau_{2j}^0 + h.o.t, \end{cases} \tag{2.10}$$

where $k_1 = Re(a_1), k_2 = Re(a_2)$.

According to [16], we obtain the following results.

Theorem 2.1 When $k_2 \neq 0$, then
1) If $k_2 < 0$, then the bifurcation periodic solutions of system (1.1) near $\tau_{2j}^0 (j = 1, 2, 3, 4)$ are stable; if $k_2 > 0$, then the bifurcation periodic solutions of system (1.1) are unstable.
2) If $k_1 k_2 < 0$, then Hopf bifurcations are supercritical; if $k_1 k_2 > 0$, then Hopf bifurcations are subcritical.

3. Numerical simulations

In this section, we will provide two numerical examples to validate our theoretical analysis.
Example 1. We consider system (1.1) with $a = -4.5, b = 1, c = 6.5, d = -2$, which satisfies the conditions (H1). Using the algorithm in [5], we obtain $\omega_2 = 7.4772, \omega_3 = 6.325, \tau_4^0 = 0.2861, \tau_6^0 = 0.2852$. From $\omega_2 = 7.4772, \tau_4^0 = 0.2861$, we get $k_1 = Re(a_1) = 0.4179 > 0$, $k_2 = Re(a_2) = -0.2349 < 0, k_1 k_2 = -0.0982 < 0$. According to Theorem 2.1, the bifurcation periodic solution of system (1.1) is stable and supercritical at $\tau = 0.4 > \tau_4^0 = 0.2861$, as shown in Figure 2. This periodic solution corresponds to the walking gait of quadrupeds.

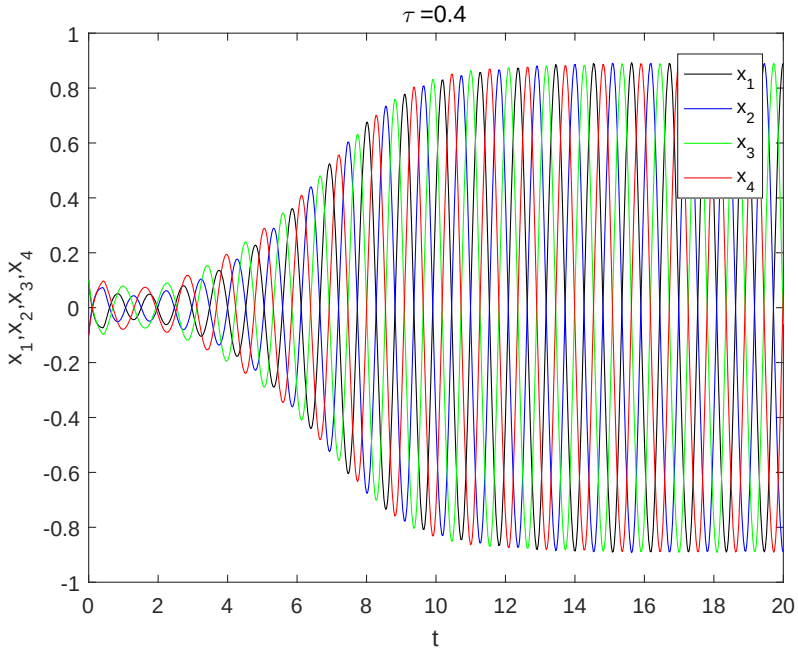

Figure 2. Trajectories $x_1(t)$, $x_2(t)$, $x_3(t)$, and $x_4(t)$ of system (1.1) when $\tau = 0.4 > \tau_4^0 = 0.2861$ with initial value (0.1,-0.1,0.1,-0.1,0.2,-0.2,0.2,-0.2).

From $\omega_3 = 6.325, \tau_6^0 = 0.2852$, we know that $k_1 = Re(a_1) = 0.6486, k_2 = Re(a_2) = -0.2544 < 0, k_1 k_2 = -0.1650 < 0$. According to Theorem 2.1, the bifurcation periodic solution of system (1.1) is stable and supercritical at $\tau = 0.4 > \tau_6^0 = 0.2852$ (see Figure 3), and this periodic solution corresponds to the trotting gait of quadrupeds.

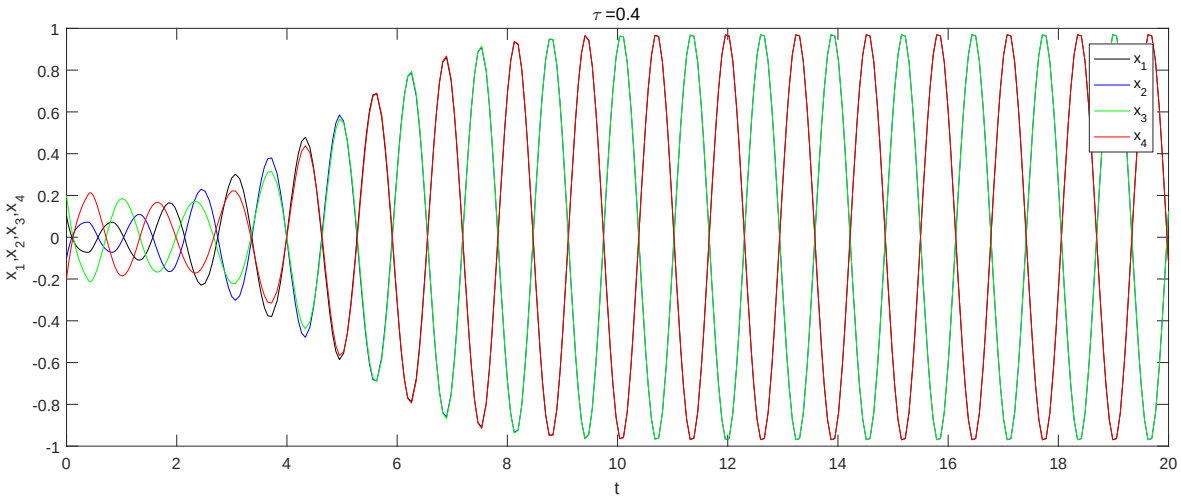

Figure 3. Trajectories $x_1(t)$, $x_2(t)$, $x_3(t)$, and $x_4(t)$ of system (1.1) when $\tau = 0.4 > \tau_6^0 = 0.2852$ with initial value (0.1,-0.1,0.2,-0.2,0.1,-0.1,0.2,-0.2).

Example 2. In system (1.1), we select parameters $a = -3, b = 0.1, c = 4, d = 1$, which satisfies

(H2). By calculation, it is obtained that $w_1 = 3.5119, \tau_2^0 = 0.5869, k_1 = Re(a_1) = 0.5957 > 0$, $k_2 = Re(a_2) = -0.5951 < 0, k_1 k_2 = -0.3545 < 0$. From Theorem 2.1, the bifurcation periodic solution of system (1.1) is stable and supercritical at $\tau = 0.7 > \tau_2^0 = 0.5869$, as shown in Figure 4. This periodic solution corresponds to the pacing gait of quadrupeds.

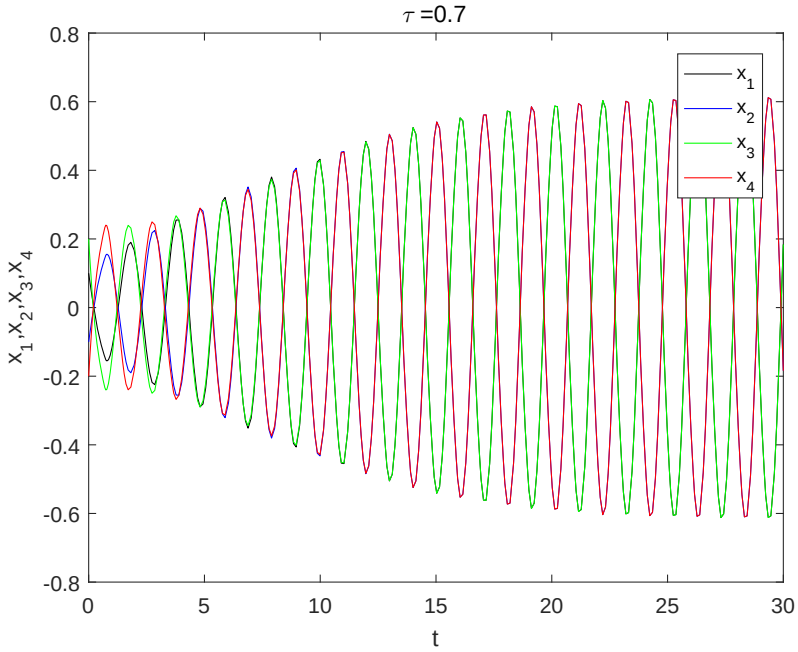

Figure 4. Trajectories $x_1(t)$, $x_2(t)$, $x_3(t)$, and $x_4(t)$ of system (1.1) with the initial values(0.1,-0.1,0.2,-0.2,0.1,-0.1,0.2,-0.2) when $\tau = 0.7$.

4. Goat gait model

In this section. we employ model (1.1) as the inversion model, and use the trust region algorithm [17] to give the goat's diagonal trotting model on flat ground and the walking gait model on the ground with a slope of 18 degrees.

4.1. Gait model for goat diagonal trotting on flat ground

By analyzing the spatiotemporal characteristic diagram of the goat's diagonal trot gait (Figure 3.2(b) in [14]), we obtain that the two legs on the diagonal of the goat are mostly in a supported or airborne state when trotting diagonally on flat ground, and the four legs airborne and single legs support the states only account for a small part of the whole gait cycle and can be ignored. So, we assume that the support state and airborne state of the two legs on the diagonal each account for half of the whole cycle. In the diagonal trotting joint angle change curve of goats (Figures 3 and 4 in [14]), an average of 20 points are extracted from the pastern joint angles and wrist joint angles curves of the two front legs, as well as the toe joint angle and tarsal joint angle curves of the two hind legs, respectively (within one cycle). Next, we translate these points to the vicinity of the origin and convert them into radians as the true values $\hat{x}_i(t_l)(i = 1, 2, \cdots, 8; l = 1, 2, \cdots, 20)$ of CPG oscillators of the corresponding legs of goats.

Finally, we averagely select 20 values of periodic solutions $x_1(t)$ to $x_8(t)$ within one cycle of model (1.1)($a = -2, b = 1, d = -2, \tau = 0.25$) as the theoretical values $x_i(t_l, c)(i = 1, 2, \cdots, 8; l = 1, 2, \cdots, 20)$ of CPG oscillators, respectively. Using the trust region algorithm [17], the parameter $c = 6.4300$ is obtained, as shown in Table 1. The error in Table 1 is $f = \frac{1}{2}\sum_{i=1}^{8}\sum_{l=1}^{20}(\hat{x}_i(t_l) - x_i(t_l, c))^2$.

Table 1. Inversion results when parameter c takes different initial values.

The initial value	Iterations	error f	Numerical solution
6.1	11	11.6591	6.4300
6.3	9	11.6591	6.4300
6.5	5	11.6591	6.4300
7.2	9	11.6591	6.4300

Next, in order to better describe the effect of the simulation, we calculated the synchronization error between the theoretical value and the real value. That is, we calculated the point-by-point difference between the 20 pairs of theoretical values and true values of the corresponding joint angles of each leg, as shown in Figures 5 and 6.

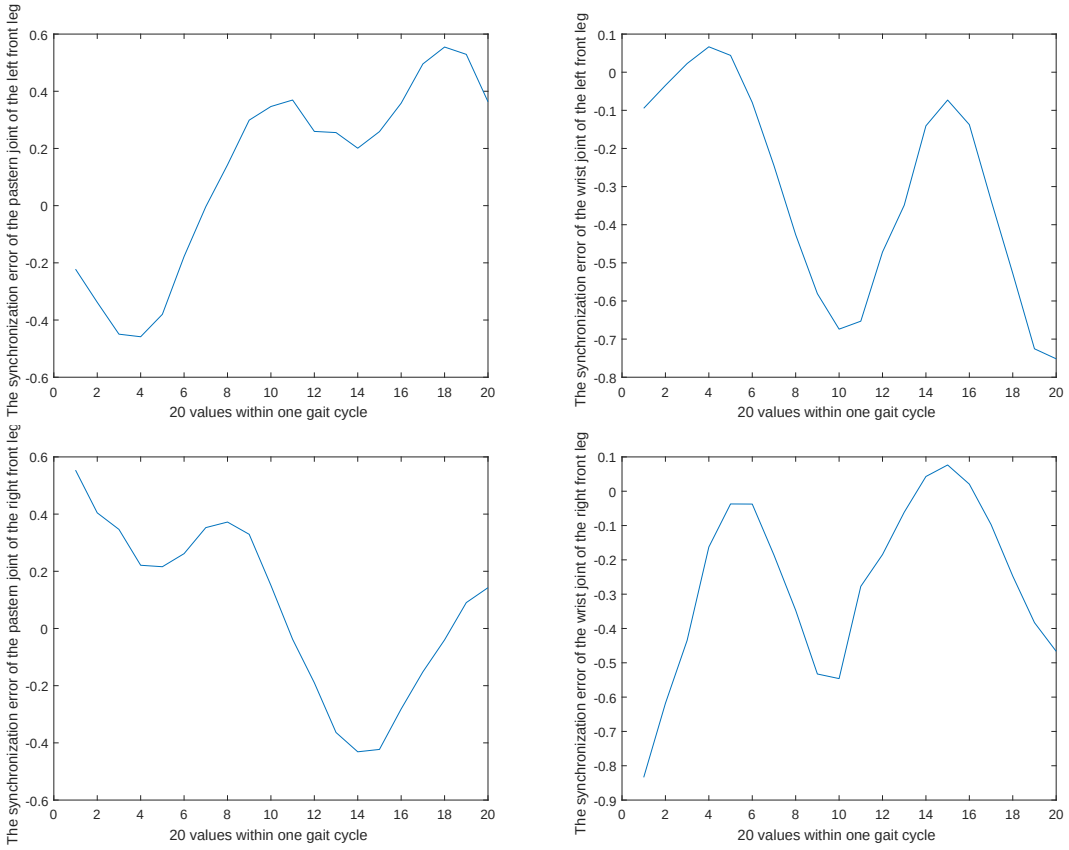

Figure 5. Schematic diagrams of synchronization error between the simulation and the real data of joint angle of front leg.

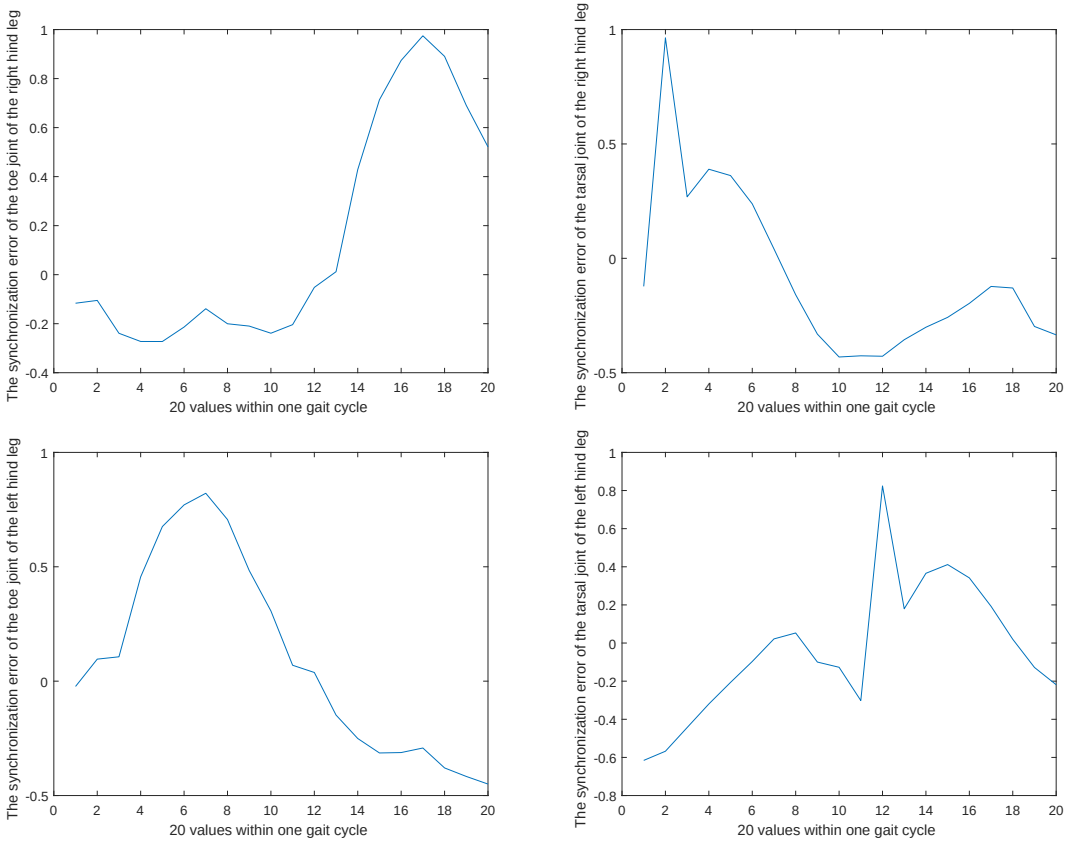

Figure 6. Schematic diagrams of synchronization error between the simulation and the real data of joint angle of hind leg.

As can be seen from Figures 5 and 6, the synchronization error ranges of the pastern joint angle and wrist joint angle of the front leg are [-0.5, 0.6] and [-0.85, 0.08], and the synchronization error ranges of the toe joint angle and the tarsal joint angle of the back leg are [-0.4, 0.95] and [-0.6, 0.95].

For parameters $a = -2, b = 1, c = 6.4300, d = -2, \tau = 0.25$, the critical value $\tau_6^0 = 0.2227$ of trotting gait and $k_1 = Re(a_1) = 1 > 0, k_2 = Re(a_2) = -0.2227 < 0, k_1 k_2 = -0.2227 < 0$ are calculated. According to Theorem 2.1, the bifurcation periodic solution of system (1.1) is stable and supercritical at $\tau = 0.25 > \tau_6^0 = 0.2227$ (see Figure 7).

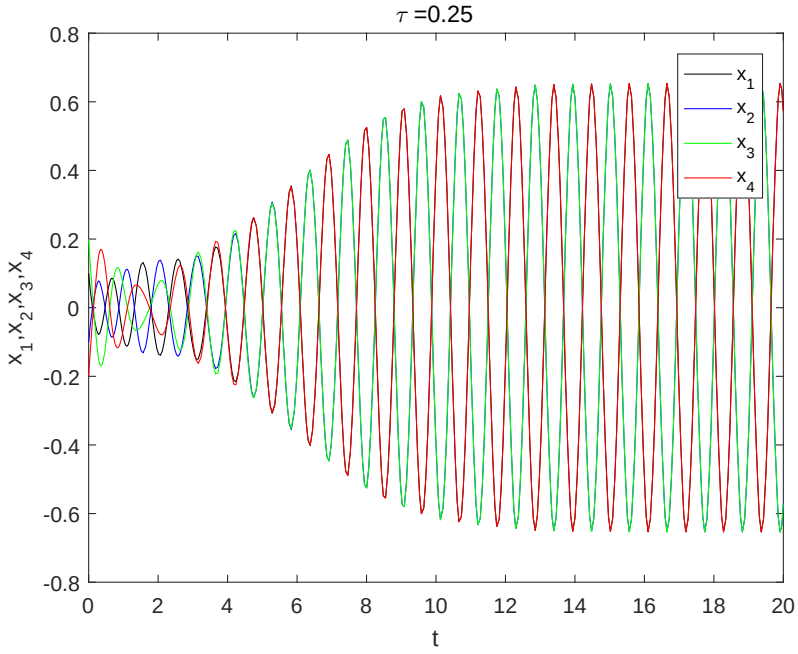

Figure 7. Trajectories $x_1(t)$, $x_2(t)$, $x_3(t)$, and $x_4(t)$ of system (1.1) with the initial values (0.1,-0.1,0.1,-0.1,0.2,-0.2,0.2,-0.2) at $\tau = 0.25$.

Therefore, the model (1.1) ($a = -2, b = 1, c = 6.4300, d = -2, \tau = 0.25$) provides a reference model for the goat's diagonal trot gait on flat ground.

4.2. Gait model of goats walking on an 18 degree slope

According to the analysis of the spatiotemporal state diagram of each leg of a goat walking on an 18 degree slope (Figures 3–8 in [15]), it is found that during one gait cycle, each leg of the goat takes turns to be suspended while the other three legs are in a supported state, and they took almost the same amount of time. Assuming that within a gait cycle, each leg of the goat is in a suspended state while the other three legs are in a supported state for the same amount of time.

Similar to Section 4.1, we take 20 data from the joint angle curve of each leg in the Figures 3–9 [15] (the curve of the wrist joint angle α of each leg and the curve of the angle β between the thighs of each leg and the forward direction) as the true values $\hat{x}_i(t_l)(i = 1, 2, \cdots, 8; l = 1, 2, \cdots, 20)$ of CPG oscillators, then we select 20 values (within one cycle) from the periodic solutions $x_1(t)$ to $x_8(t)$ of the model (1.1)$(a = -2, b = 1, c = 6.5, d = -2)$ as the theoretical values $x_i(t_l, \tau)(i = 1, 2, \cdots, 8; l = 1, 2, \cdots, 20)$ of CPG oscillators, and the parameter $\tau = 0.2450$ is obtained by the trust region algorithm, as shown in Table 2. The precision ε in Table 2 is the degree of accuracy that the gradient of the objective function $f = \frac{1}{2}\sum_{i=1}^{8}\sum_{l=1}^{20}(\hat{x}_i(t_l) - x_i(t_l, \tau))^2$ needs to achieve when the objective function f reaches its optimal solution in the trust region algorithm. Similar to Section 4.1, synchronization error diagrams between theoretical values and true values are shown in Figures 8 and 9.

Table 2. Inversion results when parameter τ takes different initial values.

The initial value of τ	Iterations	precision ε	Numerical solution
0.25	5	1.85	0.2450
0.28	8	1.85	0.2450
0.39	16	1.85	0.2450
0.4	13	1.85	0.2450

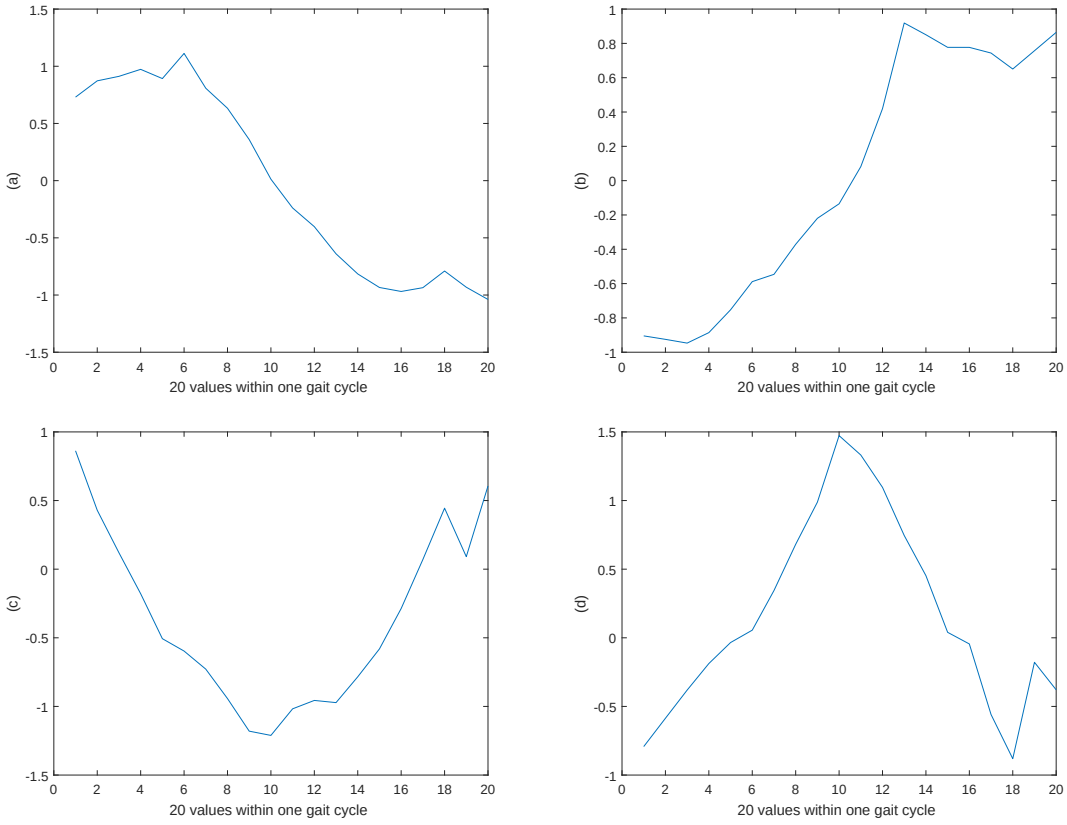

Figure 8. Schematic diagrams of synchronization error between simulation and real data of the wrist joint of legs: (a) left hind leg; (b) right hind leg; (c) left front leg; (d) right front leg.

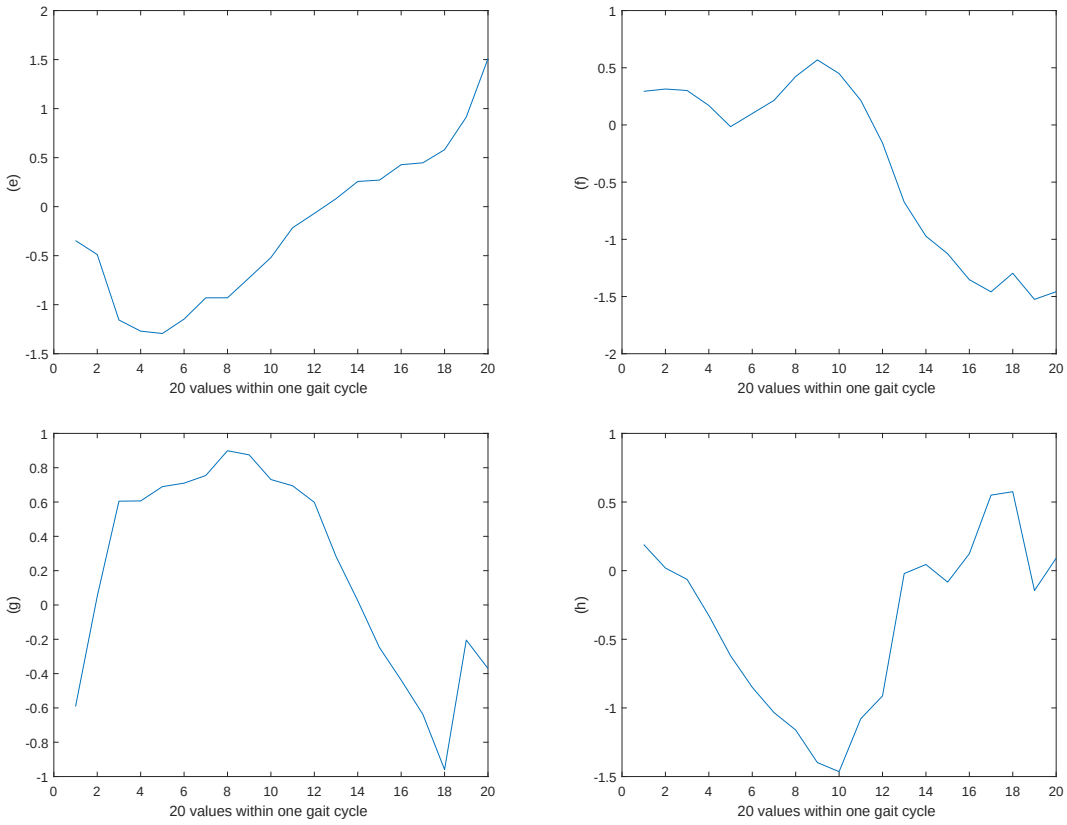

Figure 9. Schematic diagrams of synchronization error between simulation and real data of the joint between the thigh and the forward direction of legs: (e) left front leg; (f) right front leg; (g) left hind leg; (h) right hind leg.

From the two figures, we see that the synchronization error ranges of the wrist angle of left hind leg, right hind leg, left front leg, and right front leg are [-1.2, 1.2], [-0.9, 0.95], [-1.2, 0.9], and [-0.9, 1.45]. The synchronization error ranges of the angle between the forward direction of thigh movement and the left hind leg, right hind leg, left front leg, and right front leg are, respectively, [-0.95, 0.9], [-1.45, 0.6], [-1.3, 1.5], and [-1.6, -0.6].

For parameters $a = -2, b = 1, c = 6.5, d = -2$, the critical values $\tau_4^0 = 0.2048$ of the walking gait and $k_1 = Re(a_1) = 0.8232 > 0, k_2 = Re(a_2) = -0.1867 < 0, k_1 k_2 = -0.1537 < 0$ are calculated. According to Theorem 2.1, the bifurcation periodic solution of system (1.1) is stable and supercritical at $\tau = 0.2450 > \tau_4^0 = 0.2048$, as shown in Figure 10.

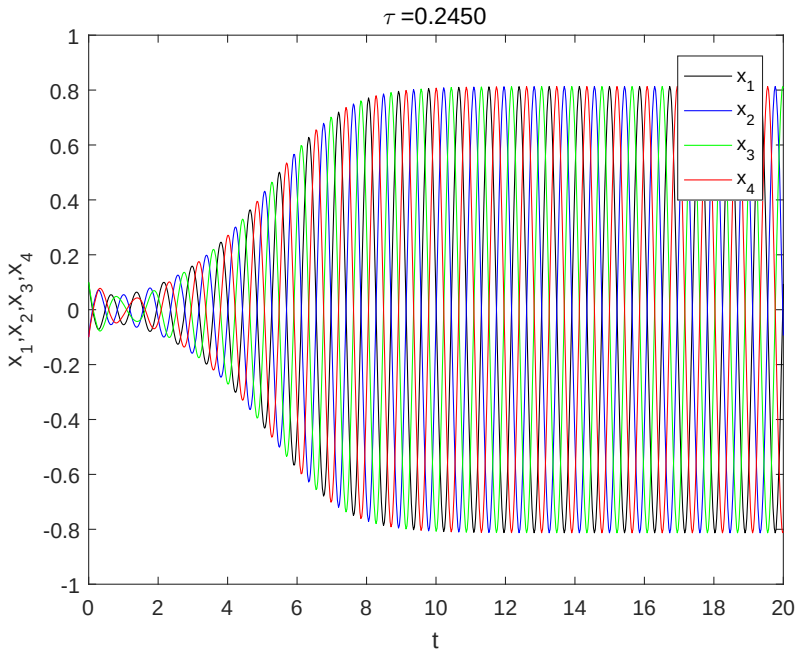

Figure 10. Trajectories $x_1(t), x_2(t), x_3(t)$, and $x_4(t)$ of system (1.1) with the initial values (0.1,-0.1,0.1,-0.1,0.2,-0.2,0.2,-0.2) at $\tau = 0.2450$.

Figure 10 indicates that the periodic solution obtained by the system (1.1) corresponds to a stable walking gait when the parameters $a = -2, b = 1, c = 6.5, d = -2, \tau = 0.2450$. Therefore, model (1.1)($a = -2, b = 1, c = 6.5, d = -2$) provides a reference model for the CPG walking gait model of goats walking uphill on an 18 degree slope when the time delay parameter $\tau = 0.2450$.

5. Conclusions

We employed the normal form theory according to Faria and Magalhães to derive the normal form for Hopf bifurcation of a quadruped gait CPG model on the center manifold, and the bifurcation direction and stability of bifurcating periodic solution at the origin are analyzed. The quadruped gait CPG model was used as an inversion model, and goat gait models were constructed using the trust region inversion algorithm. The feasibility of using the CPG model as a goat gait model was verified through simulations.

The neural network model presented in this article can predict the goat gait to contribute to artificial intelligence. The weakness of this paper is that the synchronization errors of some points are slightly larger when using our mathematical model to simulate goat gait, especially walking gait. We will modify this model further in the future.

Use of AI tools declaration

The authors declare they have not used Artificial Intelligence (AI) tools in the creation of this article.

Acknowledgments

This research is supported by the Fundamental Research Funds for the Central Universities, (No.2572022DJ08).

Conflict of interest

The authors declare there is no conflict of interest.

References

1. M. Golubitsky, I. Stewart, P. Buono, J. Collins, Symmetry in locomotor central pattern generators and animal gaits, *Nature*, **401** (1999), 693–695. https://doi.org/10.1038/44416
2. P. Buono, M. Golubitsky, Models of central pattern generators for quadruped locomotion. I. Primary gaits, *J. Math. Biol.*, **42** (2001), 291–326. https://doi.org/10.1007/s002850000058
3. P. Buono, Models of central pattern generators for quadruped locomotion. II.Secondary gaits, *J. Math. Biol.*, **42** (2001), 327–346. https://doi.org/10.1007/s002850000073
4. L. Q. Liu, C. R. Zhang, Dynamic properties of VDP-CPG model in rhythmic movement with delay, *Math. Biosci. Eng.*, **17** (2020), 3190–3202. https://doi.org/10.3934/mbe.2020181
5. L. Q. Liu, X. X. Liu, C. R. Zhang, Realization of neural network for gait characterization of quadruped locomotion, *J. Appl. Anal. Comput.*, **12** (2022), 455–463. https://doi.org/10.11948/20210005
6. B. Strohmer, P. Manoonpong, L. B. Larsen, Flexible spiking CPGs for online manipulation during hexapod walking, *Front. Neurorobotics*, **14** (2020), 1–12. https://doi.org/10.3389/fnbot.2020.00041
7. C. Bal, Neural coupled central pattern generator based smooth gait transition of a biomimetic hexapod robot, *Neurocomputing*, **420** (2021), 210–226. https://doi.org/10.1016/j.neucom.2020.07.114
8. Y. Son, T. Kamano, T. Yasuno, T. Suzuki, H. Harada, Generation of adaptive gait patterns for quadruped robot with CPG network including motor dynamic model, *Electr. Eng. Jpn.*, **155** (2006), 35–43. https://doi.org/10.1002/eej.20225
9. T. T. Duc, I. M. Koo, Y. H. Lee, H. Moon, S. Park, J. C. Koo, et al., Central pattern generator based reflexive control of quadruped walking robots using a recurrent neural network, *Robot. Auton. Syst.*, **62** (2014), 1497–1516. https://doi.org/10.1016/j.robot.2014.05.011
10. J. Q. Zhang, F. Gao, X. L. Han, X. B. Chen, X. Y. Han, Trot gait design and CPG method for a quadruped robot, *J. Bionic. Eng.*, **11** (2014), 18–25. https://doi.org/10.1016/S1672-6529(14)60016-0
11. J. X. Zhao, T. Iwasaki, CPG control for harmonic motion of assistive robot with human motor control identification, *IEEE Trans. Control Syst. Technol.*, **28** (2020), 1323–1336. https://doi.org/10.1109/TCST.2019.2910160

12. H. Suzuki, H. Nishi, Animal gait generation based on human feeling for quadrupedal robot, *Int. J. Innovative Comput., Inf. Control*, **4** (2008), 3341–3348.

13. Z. Bhatti, Oscillator driven central pattern generator (CPG) system for procedural animation of quadruped locomotion, *Multimedia Tools Appl.*, **78** (2019), 30485–30502. https://doi.org/10.1007/s11042-019-7641-1

14. Y. J. Xu, *Analysis and Simulation of Kinematic Characteristics of Goat's Multi-mode Gait*, Masters Thesis, Jilin University, 2021. https://doi.org/10.27162/d.cnki.gjlin.2021.005610

15. G. Y. Zhang, *Research on Bionic Goat Mechanism on Sloping Fields*, Masters Thesis, Henan University of Science and Technolog, 2011.

16. T. Faria, L. T. Magalhães, Normal forms for retarded functional differential equation with parameters and applications to hopf bifurcation, *J. Differ. Equations*, **122** (1995), 181–200. https://doi.org/10.1006/jdeq.1995.1144

17. T. Min, Y. Cheng, M. L. Gu, H. H. You, Parameter estimation of nonlinear dynamic system and sensitivity, *Comput. Eng. Appl.*, **49** (2013), 47–49. https://doi.org/10.3778/j.issn.1002-8331.1110-0488

AIMS Press